HHS Public Access

Author manuscript

Dev Biol. Author manuscript; available in PMC 2023 June 18.

Published in final edited form as:

Dev Biol. 2022 May ; 485: 61–69. doi:10.1016/j.ydbio.2022.02.008.

Arid1a regulates bladder urothelium formation and maintenance

Chunming Guo[a], **Yingsheng Zhang**[a], **Ruirong Tan**[a], **Zonghao Tang**[a], **Christa M. Lam**[a], **Xing Ye**[a], **Zhong Wang**[b], **Xue Li**[a,*]

[a]Samuel Oschin Comprehensive Cancer Institute, Department of Medicine, Department of Biomedical Sciences, Cedars-Sinai Medical Center, 8700 Beverly Blvd, Davis 3089, Los Angeles, CA, 90048, USA

[b]Department of Cardiac Surgery Cardiovascular Research Center, University of Michigan, Ann Arbor, MI, 48109, USA

Abstract

Epigenetic regulation of gene expression plays a central role in bladder urothelium development and maintenance. ATPase-dependent chromatin remodeling is a major epigenetic regulatory mechanism, but its role in the bladder has not been explored. Here, we show the functions of *Arid1a,* the largest subunit of the SWI/SNF or BAF chromatin remodeling ATPase complex, in embryonic and adult bladder urothelium. Knockout of *Arid1a* in urothelial progenitor cells significantly increases cell proliferation during bladder development. Deletion of *Arid1a* causes ectopic cell proliferation in the terminally differentiated superficial cells in adult mice. Consistently, gene-set enrichment analysis of differentially expressed genes demonstrates that the cell cycle-related pathways are significantly enriched in *Arid1a* knockouts. Gene-set of the polycomb repression complex 2 (PRC2) pathway is also enriched, suggesting that *Arid1a* antagonizes the PRC2-dependent epigenetic gene silencing program in the bladder. During acute cyclophosphamide-induced bladder injury, *Arid1a* knockouts develop hyperproliferative and hyperinflammatory phenotypes and exhibit a severe loss of urothelial cells. A Hallmark gene-set of the oxidative phosphorylation pathway is significantly reduced in *Aria1a* mutants before injury and is unexpectedly enriched during injury response. Together, this study uncovers functions of *Arid1a* in both bladder progenitor cells and the mature urothelium, suggesting its critical roles in urothelial development and regeneration.

Keywords

Bladder; Urothelium; Regeneration; Epigenetics; SWI/SNF; ARID1A; PRC2

1. Introduction

The bladder urothelium is a quiescent epithelial tissue of the bladder lumen that functions to prevent urine leakage into underlying tissues. Mature bladder urothelium consists of three

*Corresponding author. sean.li@cshs.org (X. Li).

Appendix A. Supplementary data

Supplementary data to this article can be found online at https://doi.org/10.1016/j.ydbio.2022.02.008.

major cell types: basal, intermediate, and superficial or umbrella cells. Although urothelial cells rarely divide, the bladder urothelium is highly regenerative in response to injuries such as urinary tract infections or chemical and physical injuries (Balsara and Li, 2017). To date, the mechanisms of bladder urothelium formation and regeneration remain poorly understood.

Post-translational modification of histones is a major epigenetic mechanism that controls gene transcription. Polycomb repressive complex 2 (PRC2)-mediated trimethylation of histone H3 lysine 27 (H3K27me3) is one such modification tightly associated with chromatin compaction and transcriptional gene silencing (Margueron and Reinberg, 2011). We have previously shown that the PRC2-dependent epigenetic program is required for bladder urothelial progenitor cell proliferation and differentiation (Guo et al., 2017). Conditional knockout of *Eed*, an obligatory subunit of PRC2, in urothelial progenitors caused premature differentiation of cytokeratin 5-positive ($Krt5^+$) basal cells and reduction of intermediate and superficial cell markers such as uroplakin 3a (*Upk3a*). Expression of other basal cell markers such as *Krt14* and *Krt17* increased in *Eed* mutant urothelium. *Cyp26a1* and *Cyp26a2*, which degrade retinoid acid (RA), were upregulated, while *Foxa1* and *Pparg* were significantly downregulated in bladder urothelium in *Eed* mutants (Guo et al., 2017). The *RA* and *Pparg* signaling pathways are critical for development of the intermediate and superficial cells (Gandhi et al., 2013; Liu et al., 2019). Formation of the basal and intermediate cells requires tumor protein p63 (*Trp63*) (Signoretti et al., 2005). These initial findings suggest that the PRC2-dependent epigenetic program promotes superficial but suppresses basal cell differentiation during bladder urothelium development.

Unlike PRC2, SWItch/Sucrose Non-Fermentable (SWI/SNF) chromatin remodeling complexes utilize energies derived from ATP hydrolysis to remodel chromatin and regulate gene transcription (Hota and Bruneau, 2016). Their function to regulate inducible genes in mating-type switching (SWI) and growth on sucrose (sucrose non-fermentable, SNF) were initially identified in yeast (Neigeborn and Carlson, 1984; Peterson and Herskowitz, 1992; Stern et al., 1984). In *Drosophila*, SWI/SNF complexes control expression of homeotic genes by antagonizing polycomb activity to determine body segment identity during development (Elfring et al., 1994; Kennison and Tamkun, 1988; Tamkun et al., 1992). Likewise, mammalian SWI/SNF and PRC2 complexes coordinately regulate gene expression in embryonic development (Kadoch et al., 2016). For example, an embryonic stem (ES) cell-specific SWI/SNF complex promotes expression of a large set of gene targets that are epigenetically silenced by PRC2 (Ho et al., 2011). Paradoxically, it also facilitates PRC2 activity to enforce transcription silencing of *Hox* genes to support ES cell pluripotency. Therefore, the two classes of epigenetic regulators, SWI/SNF and PRC2, function both antagonistically and synergistically in ES cells.

AT-rich interactive domain-containing protein 1A, *Arid1a* (also known as *Baf250a*), is the largest subunit of SWI/SNF also known as Brg-/Brama-associated factor (BAF) chromatin remodeling complexes (Gao et al., 2008; Nie et al., 2000; Wilsker et al., 2005). Mouse *Arid1a* is broadly expressed throughout embryonic development. Knockout of mouse *Arid1a* severely compromises pluripotency of ES cells and causes developmental arrest of mouse embryos (Gao et al., 2008). Somatic mutations of human *ARID1A* are frequently

observed in cancers such as urothelial carcinoma of the bladder (Robertson et al., 2017). However, the physiological role of *Arid1a* in bladder urothelial cells remains elusive. In this study, we use two *Arid1a* conditional knockout mouse alleles to investigate functions of *Arid1a* in progenitor and mature urothelial cells. We provide evidence suggesting that *Arid1a* maintains the differentiated state of the urothelium and antagonizes the PRC2-dependent epigenetic gene silencing program. We also show that *Arid1a* regulates oxidative phosphorylation during bladder urothelium development and regeneration.

2. Results

2.1. Arid1a is enriched in terminally differentiated superficial cells

In adult mouse bladders, immunofluorescence analysis of ARID1A protein distribution showed that it is broadly distributed in all three layers of the developing bladder at the onset of bladder cell differentiation at embryonic day 13.5 (E13.5) (Fig. 1A). ARID1A was also detected in adult bladder at postnatal day 60 (P60); and appeared to be enriched in cells facing bladder lumen. A punctate nucleus staining pattern was observed throughout all layers of the bladder, including cells of the smooth muscle, lamina propria, and urothelium (Fig. 1A). Co-immunostaining with a superficial cell marker Uroplakin 3a (*Upk3a*) indicated that superficial cells at the luminal surface displayed much stronger signals compared to other cell types (Fig. 1B).

To further examine the expression of *Arid1a* and other components of SWI/SNF complexes in the developing urothelium, we used a Translating Ribosome Affinity Purification (TRAP) strategy (Zhou et al., 2013) to isolate urothelium-specific mRNA at embryonic day 15.5 (E15.5), 18.5 (E18.5) and postnatal day 60 (P60) (Figure s1). The TRAP technology utilizes a genetic strategy to tag and isolate cell type-specific mRNAs without physically dissociating and purifying the cell type-of-interests from their native environment (Zhou et al., 2013). Specifically, we used Shh^{GC} Cre-driver (Guo et al., 2017) and $R26R^{TRAP}$ conditional allele (Zhou et al., 2013) to selectively activate expression of L10a-GFP fusion gene in the urothelial cells (Figure s1A). During translation of mRNAs, L10a-GFP is incorporated into the polysome, which permits co-immunoprecipitation and isolation of the polysome-bound mRNA using an GFP-specific antibody (Zhou et al., 2013). The bladders of $Shh^{GC};R26R^{TRAP}$ at various developmental stages were used for the co-immunoprecipitation assay to isolate mRNAs selectively from the urothelial cells. RNA-seq of the resulting urothelium-specific TRAP RNAs confirmed that *Arid1a, Arid1b, Brg1/Smarca4 and Baf47/Smarcb1* were expressed in the urothelium of all developmental stages (Figure s1B). Expression of *Arid1a* and *Arid1b* appeared to be lower at E18.5 and p60 when compared to E15.5. *Baf47* also displayed a similar trend of diminished expression as development progresses. These findings are consistent with the potential roles of SWI/SNF complexes in urothelium development.

2.2. Arid1a gene deletion is associated with hyperproliferation and aberrant differentiation

To examine the function of *Arid1a* in the development of bladder urothelium, we deleted *Arid1a* gene in all urothelial progenitor cells by intercrossing a floxed *Arid1a* allele

(*Arid1a*$^{F/F}$) (Gao et al., 2008) with an *Shh*^{GC} allele (Harfe et al., 2004); the latter expresses an elf and Cre fusion protein (GC) via the endogenous *Shh* locus in. We previously reported that *Shh*^{GC} is an effective *Cre*-driver to conditionally delete floxed genes in urothelial progenitors and all urothelial cell lineages (Guo et al., 2017). As expected, the resulting compound mutants, *Arid1a*$^{F/F}$;*Shh*$^{GC/+}$ or *Arid1a*^{Shh}, had no detectable ARID1A protein in the urothelium (Fig. 1C). Expression of *Arid1a* in the bladder smooth muscle and lamina propria layers was not affected in the mutants. Successful deletion of *Arid1a* was further confirmed by quantitative reverse transcription polymerase chain reaction (qRT-PCR) assay using micro-dissected bladder urothelium. *Arid1a* transcripts were significantly lower in the mutants when compared to heterozygous controls (Fig. 1D). Expression of *Arid1b*, a paralog of *Arid1a* and a mutually exclusive subunit of SWI/SNF complexes, was significantly upregulated in the mutants (Fig. 1D), suggesting that *Arid1a* suppresses *Arid1b* expression and upregulation of *Arid1b* may compensate the loss of *Arid1a* in the bladder urothelium.

In *Arid1a*^{Shh} embryos, the bladder urothelium appeared to be disorganized based on nuclear DAPI (4′,6-diamidino-2-phenylindole) staining (Fig. 1C). Specifically, the mutant urothelium lacked a stratified appearance as observed in controls, and its basal layer consisted of numerous disorganized small nuclei. This observation was confirmed by a histological staining shown in Fig. 2A. The apical surface of urothelial cells in *Arid1a*^{Shh} mutants appeared to be less defined and uniform compared to controls, suggesting that *Arid1a* might be required for differentiation and/or maturation of the superficial cells. *Arid1a*^{Shh} mutant urothelium had significantly more proliferating cells as indicated by increased Ki67-and phospho-histone H3 (pHH3)-positive cells (Fig. 2B–D). Interestingly, high levels of Ki67^{+} and pHH3^{+} proliferating cells were observed in not only the urothelium but also the lamina propria layer (Fig. 2B and C). Since *Arid1a* was only deleted in the urothelial cells, these observations suggest that *Arid1a* has both intrinsic and extrinsic effects in inhibiting cell proliferation in the urothelium and the lamina propria layers, respectively.

To further investigate a potential role of *Arid1a* in urothelial cell differentiation, we examined expression of genes enriched in the superficial and basal cells. The overall KRT5 and UPK3A-specific immunostaining patterns were comparable in bladder urothelium between the mutants and controls (Fig. 3A and B). The KRT5-positive cells were at the basal layer of the urothelium and the UPK3A-positive cells located at the luminal surface. There was a clear gap between the KRT5-and UPK3A-positive layers in the urothelium control. This gap was diminished in the mutant urothelium (Fig. 3B). Consistent with the histological observations (Fig. 2A and C), there were significantly fewer UPK3A^{+} superficial cells observed in *Arid1a*^{Shh} mutants (Fig. 3C). We have also observed that the increase of Ki67 positive cells was primarily restricted to the UPK3A-negative cell population (Fig. 3D and E), suggesting the basal cells instead of the superficial cells were hyper-proliferative in *Arid1a*^{Shh} mutants during development (Fig. 3D and E). Basal cell markers including *Krt14* and *Krt17* were also increased (Fig. 3F). Transcription factors important for urothelial cell differentiation, such as *Trp63* and *Pparg*, were down-regulated in the mutants (Fig. 3G). Levels of *Krt5*, *Krt20* and *Upk2* were not affected in *Arid1* mutants. These observations collectively suggest that loss-of-*Arid1a* causes dysregulation of transcription of genes important for cell proliferation and differentiation during bladder urothelium development.

2.3. Ectopic expression of Ezh2 in the adult bladder urothelium of Arid1a mutants

Since *Shh*^{GC} Cre driver is also active in other tissues such as lung epithelial progenitors (Guo et al., 2017), *Arid1a* was also deleted in the lungs of *Arid1a*^{Shh} embryos. All *Arid1a*^{Shh} mutant embryos were dead at birth with an apparent hypoplastic lung defect, suggesting this mutation is incompatible with life (Figure s1). Compared with littermate heterozygous controls, the mutant lungs were translucent and small (), a likely reason for embryonic lethality of *Arid1a*^{Shh} mutants. Mutant bladders and ureters were grossly normal (Figures s1B and C). Hydronephrosis was occasionally observed (Figure s1D).

To circumvent the perinatal lethal phenotype and examine the role of *Arid1a* in mature bladder urothelium, we used a different Cre driver, *Upk2-Cre* (Guo et al., 2017), to specifically delete *Arid1a* in the urothelium. Immunostaining with an ARID1A-specific antibody demonstrated an efficient deletion in the urothelium of *Arid1a*$^{F/F}$*;Upk2-Cre* or *Arid1a*^{Upk2} mice (Fig. 4A). The KRT5-and UPK3A-specific staining patterns were comparable between mutants and littermate heterozygous controls (Fig. 4B). However, there were significantly more Ki67-positive cells in *Arid1a*^{Upk2} mutants. This finding is consistent with the inhibiting function of *Arid1a* in embryonic urothelial cell proliferation. Interestingly, Ki67-positive cells were located at the luminal surface of bladder urothelium (Fig. 5C). This was unexpected because the basal but not superficial cells exhibited hyperproliferation in *Arid1a*^{Shh} mutants (Fig. 3). These findings suggest that while *Arid1a* is clearly important in regulating urothelial cell proliferation, it may play different roles in the developing and mature urothelium. An increase in cell cycle in mature urothelium implies that *Arid1a* is required to maintain the terminally differentiated state, such as polyploidy of superficial cells (Wang et al., 2018).

To investigate the potential role of *Arid1a* in regulating gene expression in bladder urothelium, we performed whole genome transcriptomic analysis of micro-dissected bladder mucosal tissue and identified a large set of differentially expressed genes (DEGs) in *Arid1a*^{Upk2} mutants using littermate heterozygous as controls (Fig. 5A and supplementary Table s1). We focused on genes related to the PRC2 epigenetic program because of its antagonistic relationship between SWI/SNF and PRC2 in gene regulation (Kadoch et al., 2016). Importantly, PRC2 is also critically involved with bladder urothelium development and regeneration (Guo et al., 2017). Among the DEGs, expression of *Ezh2*, which encodes the methyltransferase of PRC2, was significantly upregulated in the mutants. This observation was confirmed by EZH2-specific immunostaining of bladder urothelium (Fig. 5B). Gene Set Enrichment Analysis (GSEA) further revealed that genes downregulated after *Ezh2* knockdown (KD) were significantly enriched in *Arid1a*^{Upk2} mutants, while genes upregulated in *Ezh2* KD cells were enriched in the control group (Fig. 5C and D). In another word, genes induced by *Ezh2* were upregulated while genes suppressed by *Ezh2* were downregulated in *Arid1a* mutants. Among the top 10 enriched Hallmark gene sets (Table 1), we found that the mitotic spindle, G2M checkpoint and E2F target gene sets were significantly enriched in *Arid1*^{Upk2} mutants. On the other hand, the p53 pathway gene set was significantly enriched. These findings were consistent with the observation of *Arid1a* regulating urothelial cell proliferation. In addition to these cell cycle related molecular pathways, gene sets that were significantly affected included UV response, protein secretion,

oxidative phosphorylation, xenobiotic metabolism, coagulation and reactive oxygen species pathway. Together, these findings suggest that *Arid1a* regulates expression of a large number of genes important to the bladder urothelium. Moreover, *Arid1a* controls gene expression, in part, by antagonizing the PRC2-dependent epigenetic repression program in the bladder.

2.4. Arid1a regulates proliferation and inflammation during bladder injury

Although relatively quiescent at steady state, the bladder urothelium is highly regenerative when injured. Both basal and intermediate cells have been implicated to regenerate superficial cells during acute or repeated urinary tract infections, surgical injuries, or chemical injuries such as those from cyclophosphamide (CPP) (Gandhi et al., 2013; Guo et al., 2017; Liu et al., 2019; Papafotiou et al., 2016; Schafer et al., 2017; Shin et al., 2011). To examine *Arid1a´s* function after acute injury, we treated adult mice with a single dose of CPP to elicit hemorrhagic cystitis and urothelium damage. As expected, CPP induced an apparent injury response of the bladder as indicated by urothelial cell proliferation and hyperplasia (Fig. 6A and B). Unlike vehicle-treated control bladders in which the urothelium was three-cell layer thick, the urothelium of CPP-treated mice had four or more cell layers. CPP exposure reactivated urothelial cell proliferation with approximated 44% Ki67-positive cells at one day-post-CPP. Cell proliferation persisted for at least three days (Fig. 6B). However, proliferation decreased dramatically by day seven, suggesting that the acute urothelial injury and repair response was near completion at this time point in the controls. Consistently, the overall inflammatory score, an indication of immune cell infiltration, edema, and loss of urothelium (Hopkins et al., 1998), was significantly higher at day 1 and 3 post-CPP than vehicle treated controls but was close to zero at 7 day-post-CPP (Fig. 6C). In comparison with heterozygous controls, the urothelium of $Arid1a^{Upk2}$ mutants appeared to be much thinner at day 1, implying severe urothelial cell loss after an acute injury (Fig. 6A). Cellularity of the mutant urothelium was comparable to the controls at 3 and 7 day-post-CPP (Fig. 6A). Urothelial hyperproliferation was detected in $Arid1a^{Upk2}$ mutants at both 3 and 7 day-post-CPP (Fig. 6B). Significantly higher inflammatory scores were also observed in the mutants at day 3 and 7 post-CPP (Fig. 6C). Altogether, these findings demonstrate that loss-of-*Arid1a* increase urothelial cell loss and also, enhances cell proliferation after an acute injury.

To identify *Arid1a*-dependent molecular pathways that were affected during CPP-induced injury response, we performed GSEA of whole genome transcriptome of micro-dissected bladder mucosa at one day-post-CPP exposure (Table 2). Gene sets closely related to inflammation such as TNFα signaling via NF-κB, inflammatory response and the IL6-JAK-STAT3 signaling pathway were significantly enriched in $Arid1a^{Upk2}$ mutants. Other gene sets including MYC targets, MTORC1 signaling, oxidative phosphorylation and reactive oxygen species were also enriched in $Arid1a^{Upk2}$ mutants. Enrichment of the oxidative phosphorylation gene set in the mutant was unexpected because this gene set was reduced in the mutants at naïve condition (Table 2). Xenobiotic metabolism, coagulation and bile acid metabolism gene sets were enriched in controls. These findings collectively suggest that *Arid1a* regulates the inflammatory response during bladder injury either directly or indirectly, and further suggest that *Arid1a* may also regulate the oxidative phosphorylation pathway in a context-dependent manner.

3. Discussion

In this study, we show that *Arid1a* is broadly expressed in the bladder urothelium during embryonic development and becomes highly enriched in terminally differentiated superficial cells of the mature urothelium. *Arid1a* inhibits proliferation in both developing and mature urothelial cells. Our findings also show that *Arid1a* functionally represses *Ezh2* gene expression, particularly in superficial cells, and antagonizes the PRC2-dependent epigenetic repression program in adult bladder urothelium. Findings here suggest that *Arid1a* is required to maintain a differentiated state of urothelial cells and further suggest that *Arid1a* plays a distinct role in urothelium development and regeneration.

We examined the potential role of SWI/SNF chromatin remodeling complexes in the bladder urothelium by selectively deleting its largest subunit *Arid1a* from the bladder urothelium. We show that expression of *Arid1b* is significantly upregulated in *Arid1a* mutants. Given that human *ARID1B* compensates for the loss of *ARID1A* in ovarian clear cell carcinoma (Trizzino et al., 2018) and *ARID1B* is a specific vulnerability in human *ARID1A*-mutant cancer cell lines (Helming et al., 2014), upregulation of *Arid1b* could compensate the loss of *Arid1a* in bladder urothelial cells. Our findings show that *Arid1a* plays an apparent role in suppressing urothelial cell proliferation in both embryonic and adult bladders. Intriguingly, we did not observe any excessive growth or dramatic thickening of the mutant urothelium. This is consistent with the observation that *ARID1A* mutations are often observed in morphologically normal human bladder urothelium (Lawson et al., 2020). Mutation of *ARID1A* is therefore unlikely to be sufficient to drive bladder tumorigenesis. Additional hits, such as seen in ovarian clear-cell tumorigenesis resulting from both *ARID1A* and *PIK3CA* mutations (Chandler et al., 2015), might be needed to drive neoplastic transformation of *ARID1A* mutant urothelium. Our studies, however, could not fully uncover the role of SWI/SNF complexes in bladder urothelium. Thus, future studies such as deleting both *Arid1a* and *Arid1b* genes are needed.

Our findings that deletion of *Arid1a* significantly increases urothelial cell proliferation is consistent with previous observations that human *ARID1A* functions as a candidate tumor suppressor and human loss-of-function mutations are closely associated with bladder cancer (Cancer Genome Atlas Research, 2014; Robertson et al., 2017). A recent study showed that *ARID1A* deficient human bladder cancer cells are more sensitive to EZH2 pharmacologic inhibition (Ferguson et al., 2021), suggesting an antagonistic relationship between *Arid1a* and *Ezh2* in urothelial cells. However, this relationship was not observed previously (Garczyk et al., 2018). In this study, we show that *Ezh2* is significantly upregulated in superficial cells of *Arid1a* mutants. *Ezh2*-activated genes are significantly enriched in *Arid1a* knockout mutants and *Ezh2*-repressed genes are enriched in heterozygous controls. Paradoxically, urothelial progenitor cell marker genes *Krt14* and *Krt17* are significantly upregulated in *Arid1a* knockouts. These genes are also upregulated in the absent of *Ezh2*-dependent PRC2 activity (Guo et al., 2017), suggesting that both *Arid1a* and *Ezh2* are required to repress expression of these genes. *Arid1a* is highly enriched in mature superficial cells. Few superficial cells were observed in *Arid1a* mutants, and they also ectopically expressed cell proliferation marker Ki67. PRC2 is also required for formation of superficial cells (Guo et al., 2017). While the precise mechanism of *Arid1a* in urothelial

cell proliferation and differentiation remains to be defined, these findings suggest a context-specific relationship between SWI/SNF and PRC2, antagonizing one another to regulate urothelial cell proliferation, but collaborating to maintain the differentiated state of bladder urothelium.

The oxidative phosphorylation pathway was among the top affected pathways after *Arid1a* gene deletion in the bladder urothelium (Table 1). Hallmark gene set of the oxidative phosphorylation pathway is reduced in *Arid1a* mutants, implying that *Arid1a* positively regulates oxidative phosphorylation in the bladder urothelium. Paradoxically, the oxidative phosphorylation pathway is enriched in *Arid1a* mutant urothelium during CPP-induced acute bladder injury (Table 2). This is unexpected because *Arid1a* inhibits the oxidative phosphorylation pathway in both lung cancer (Deribe et al., 2018) and clear cell carcinoma of the ovaries (Zhang et al., 2021). *Arid1a* mutants exhibit an enhanced inflammatory host responsive to CPP-induced bladder injury. Despite substantial loss of urothelial cells at one day post-CPP, the mutant urothelium appear to recover substantially at 7 day-post-CPP. Since the initial severe cell loss could expose bladder tissue to chemical irritants in the urine, it is possible that the inflammatory host response is due to the loss-of-*Arid1a* in the urothelium, a breach in the urothelial barrier or both. The precise mechanism underlying *Arid1a*-dependent urothelial regeneration remains unclear, however, our study suggests that *Arid1a* functions antagonistically against the PRC2-dependent epigenetic repression program. Previous studies have shown that *Arid1a* deletion accelerates regeneration of the liver (Sun et al., 2016). In contrast, a different study reported that *Arid1a* promotes a permissive chromatin state and facilitates expression of liver-progenitor-like cell genes in response to liver injury and repair (Li et al., 2019). Therefore, it is likely that the function of *Arid1a* is context-dependent and may play opposite roles in development, maintenance and pathogenesis of bladder urothelium.

4. Materials and methods

4.1. Mouse strains

Arid1a$^{F/F}$ floxed allele (Jackson Laboratory, 027717) was generously provided by Dr. Zhong Wang (Gao et al., 2008). Urothelium-specific *Arid1a* knockout mouse lines were generated using the same strategies that we previously described in detail (Guo et al., 2017). Briefly, we intercrossed *Arid1a*$^{F/F}$ allele with Cre drivers *Upk2*-Cre (Guo et al., 2017) and *Shh*^{GC} (Harfe et al., 2004) to conditionally delete *Arid1a* before and after bladder organogenesis, respectively. Heterozygous littermate mutants were used as controls. All animal studies using both males and females were performed according to protocols reviewed and approved by the Institutional Animal Care and Use Committee at Boston Children's Hospital and Cedars-Sinai Medical Center.

4.2. Histology, immunostaining and bladder injury

Histology and immunostaining were performed as previously described (Guo et al., 2017). For CPP induced bladder injuries, adult male mice (2 to 4-month-old) were intraperitoneally injected with a single dose of CPP (150 μg/g body weight in PBS, Sigma C7397). Analyses were performed at 1, 3 and 7 day-post-injection. Inflammatory scores were graded using

criteria described by Hopkins et al. (1998), and scored blinded to all treatment groups. Grade 1: subepithelial cell inflammatory infiltration (either focal or multifocal); Grade 2, edema and diffused subepithelial inflammatory cell infiltration; Grade 3, marked subepithelial inflammatory cells with necrosis and neutrophils in and on bladder mucosal epithelium; Grade 4, inflammatory cell infiltrate extends into muscle in addition to criteria for Grade 3; Grade 5, loss of surface epithelium (necrosis with full-thickness inflammatory cell infiltration). Antibodies used for immunostaining include ARID1A (1:100 Cell signaling Technology,12354), Ki67 (1:100 Abcam 16667), pHH3 (1:100 Millipore, 06–570), KRT5 (1:500 Abcam, ab53121; 1:500, Covance, SIG-3475) and UPK3A (1:200 provided by Dr. T.T. Sun).

4.3. Translating Ribosome Affinity Purification (TRAP)

Shh^{GC} Cre-driver (Guo et al., 2017) and *R26R*^{TRAP} conditional allele (Zhou et al., 2013) were used to selectively activate expression of L10a-GFP fusion gene in the urothelial cells. TRAP mRNA purification was done essentially as described (Heiman et al., 2014). About 100 mg of pooled various staged bladder tissues (E15.5, E18.5, and P60) were used in the co-immunoprecipitation using an GFP antibody (Zhou et al., 2013) to isolate the polysome-bound mRNAs. TRAP RNAs was sequenced using Illumina 2500 platform (20 million reads/sample of pair-end 150). Pathway analysis was done using both the Ingenuity Pathway Analysis and Gene Set Enrichment Analysis.

4.4. RNA isolation, RNA-seq and qRT-qPCR

RNeasy RNA isolation kit (Qiagen) was used to isolate total RNA from micro-dissected bladder urothelium from 2 to 4-month-old mice. Genomic DNA was removed using gDNA Eliminator spin columns (Qiagen). RNA-seq of the isolated RNAs was done using Illumina 2500 platform (20M, PE150). Cutoff for differentially expressed genes (DEGs) was based on log2 [Fold change (Mutant/WT)] >1 or < −1 and p (adj) < 0.05. For quantitative real-time PCR (qRT-PCR) experiments, mRNA was reverse-transcribed into cDNA using the SuperScript® III Reverse Transcriptase Kit (Invitrogen). qRT-PCR analyses were performed using SYBR Green (Roche) on an ABI-7500 detector (Applied BioSystems). Relative gene expression levels were normalized to the internal control *Gapdh*. The following gene-specific primers were used: *Arid1a*: 5′-GGC CAC AAA CTC CTC AGT CA and 5′-GAC TGA GTT GCT CCT GCT CA; *Arid1b*: 5′-GGC CGT CTC GGA GTT TAA TA and 5′-CAT CGG GCT GCC CTG G; *Trp63*: 5′-AGA ACG GCG ATG GTA CGA AG and 5′-TCT CAC GAC CTC TCA CTG GT; *Pparg*: 5′-ATT GAG TGC CGA GTC TGT GG and 5′-GCC CAA ACC TGA TGG CAT TG; Upk1b: 5′-ACG CGA CTT TTT CAC AAC CA and 5′-CTG ACG GAC CGT TTA CAC CA; *Upk2*: 5′-CAT GTC CAC GCT TCC TCG AAA and 5′-AGA CCC ACG ACC AAC AGG AA; *Upk3a*: 5′-GAT CCC ATC TGG ACC AAC CG and 5′-CCC ATG TCC ACA AAG CTG AGG; *Upk3b*: 5′-GAG ACG AAG TGG TCC AAC CC and 5′-CCT TCC CCA CTC AGC; *Krt14*: 5′-AGG AGA CCA AAG GCC GTT AC and 5′-GGT TGG TGG AGG TCA CAT CTC; *Krt20*: 5′-GTC CCA CCT CAG CAT GAA AGA and 5′-TCT GGC GTT CTG TGT CAC TC; *Krt17*: 5′-TCC CAG CTC AGC ATG AAA GC and 5′-CTT GTA CTG AGT CAG GTG GGC.

4.5. Statistical analysis

For all graphs, data are presented as the mean value ± SEM. Student's *t*-test was used to determine significance between two groups. P values < 0.05 were considered statistically significant.

Supplementary Material

Refer to Web version on PubMed Central for supplementary material.

Acknowledgments

We thank all members of the X.L. lab, particularly Dr. Satoshi Kaneko for technical supports and helpful discussions. This work was supported by NIH/NIDDK (R01DK110477 and U01DK131377, X.L.), NIH/NCI (R21CA249701, X.L) and NHLBI (1R01HL136921, X.L.).

References

Balsara ZR, Li X, 2017. Sleeping beauty: awakening urothelium from its slumber. Am. J. Physiol. Ren. Physiol 312, F732–F743.

Cancer Genome Atlas Research, N., 2014. Comprehensive molecular characterization of urothelial bladder carcinoma. Nature 507, 315–322. [PubMed: 24476821]

Chandler RL, Damrauer JS, Raab JR, Schisler JC, Wilkerson MD, Didion JP, Starmer J, Serber D, Yee D, Xiong J, Darr DB, Pardo-Manuel de Villena F, Kim WY, Magnuson T, 2015. Coexistent ARID1A-PIK3CA mutations promote ovarian clear-cell tumorigenesis through pro-tumorigenic inflammatory cytokine signalling. Nat. Commun. 6, 6118. [PubMed: 25625625]

Deribe YL, Sun Y, Terranova C, Khan F, Martinez-Ledesma J, Gay J, Gao G, Mullinax RA, Khor T, Feng N, Lin YH, Wu CC, Reyes C, Peng Q, Robinson F, Inoue A, Kochat V, Liu CG, Asara JM, Moran C, Muller F, Wang J, Fang B, Papadimitrakopoulou V, Wistuba II, Rai K, Marszalek J, Futreal PA, 2018. Author Correction: mutations in the SWI/SNF complex induce a targetable dependence on oxidative phosphorylation in lung cancer. Nat. Med. 24, 1627.

Elfring LK, Deuring R, McCallum CM, Peterson CL, Tamkun JW, 1994. Identification and characterization of Drosophila relatives of the yeast transcriptional activator SNF2/SWI2. Mol. Cell Biol. 14, 2225–2234. [PubMed: 7908117]

Ferguson JE, Rehman H, Chandrashekar DS, Chakravarthi BVSK, Nepal S, Eich M-L, Robinson AD, Agarwal S, Hodigere Balasubramanya SA, Naik G, Manne U, Netto GJ, Pan C. x., Sonpavde G, Varambally S, 2021. ARID1A-mutant and deficient bladder cancer is sensitive to EZH2 pharmacologic inhibition. bioRxiv, 2021 426383, 2001.2012.

Gandhi D, Molotkov A, Batourina E, Schneider K, Dan H, Reiley M, Laufer E, Metzger D, Liang F, Liao Y, Sun TT, Aronow B, Rosen R, Mauney J, Adam R, Rosselot C, Van Batavia J, McMahon A, McMahon J, Guo JJ, Mendelsohn C, 2013. Retinoid signaling in progenitors controls specification and regeneration of the urothelium. Dev. Cell 26, 469–482. [PubMed: 23993789]

Gao X, Tate P, Hu P, Tjian R, Skarnes WC, Wang Z, 2008. ES cell pluripotency and germ-layer formation require the SWI/SNF chromatin remodeling component BAF250a. Proc. Natl. Acad. Sci. U. S. A. 105, 6656–6661. [PubMed: 18448678]

Garczyk S, Schneider U, Lurje I, Becker K, Vogeli TA, Gaisa NT, Knuchel R, 2018. ARID1A-deficiency in urothelial bladder cancer: No predictive biomarker for EZH2-inhibitor treatment response? PLoS One 13, e0202965. [PubMed: 30138427]

Guo C, Balsara ZR, Hill WG, Li X, 2017. Stage- and subunit-specific functions of polycomb repressive complex 2 in bladder urothelial formation and regeneration. Development 144, 400–408. [PubMed: 28049658]

Harfe BD, Scherz PJ, Nissim S, Tian H, McMahon AP, Tabin CJ, 2004. Evidence for an expansion-based temporal Shh gradient in specifying vertebrate digit identities. Cell 118, 517–528. [PubMed: 15315763]

Heiman M, Kulicke R, Fenster RJ, Greengard P, Heintz N, 2014. Cell type-specific mRNA purification by translating ribosome affinity purification (TRAP). Nat. Protoc. 9, 1282–1291. [PubMed: 24810037]

Helming KC, Wang X, Wilson BG, Vazquez F, Haswell JR, Manchester HE, Kim Y, Kryukov GV, Ghandi M, Aguirre AJ, Jagani Z, Wang Z, Garraway LA, Hahn WC, Roberts CW, 2014. ARID1B is a specific vulnerability in ARID1A-mutant cancers. Nat. Med. 20, 251–254. [PubMed: 24562383]

Ho L, Miller EL, Ronan JL, Ho WQ, Jothi R, Crabtree GR, 2011. esBAF facilitates pluripotency by conditioning the genome for LIF/STAT3 signalling and by regulating polycomb function. Nat. Cell Biol. 13, 903–913. [PubMed: 21785422]

Hopkins WJ, Gendron-Fitzpatrick A, Balish E, Uehling DT, 1998. Time course and host responses to Escherichia coli urinary tract infection in genetically distinct mouse strains. Infect. Immun. 66, 2798–2802. [PubMed: 9596750]

Hota SK, Bruneau BG, 2016. ATP-dependent chromatin remodeling during mammalian development. Development 143, 2882–2897. [PubMed: 27531948]

Kadoch C, Copeland RA, Keilhack H, 2016. PRC2 and SWI/SNF chromatin remodeling complexes in health and disease. Biochemistry 55, 1600–1614. [PubMed: 26836503]

Kennison JA, Tamkun JW, 1988. Dosage-dependent modifiers of polycomb and antennapedia mutations in Drosophila. Proc. Natl. Acad. Sci. U. S. A. 85, 8136–8140. [PubMed: 3141923]

Lawson ARJ, Abascal F, Coorens THH, Hooks Y, O'Neill L, Latimer C, Raine K, Sanders MA, Warren AY, Mahbubani KTA, Bareham B, Butler TM, Harvey LMR, Cagan A, Menzies A, Moore L, Colquhoun AJ, Turner W, Thomas B, Gnanapragasam V, Williams N, Rassl DM, Vohringer H, Zumalave S, Nangalia J, Tubio JMC, Gerstung M, Saeb-Parsy K, Stratton MR, Campbell PJ, Mitchell TJ, Martincorena I, 2020. Extensive heterogeneity in somatic mutation and selection in the human bladder. Science 370, 75–82. [PubMed: 33004514]

Li W, Yang L, He Q, Hu C, Zhu L, Ma X, Ma X, Bao S, Li L, Chen Y, Deng X, Zhang X, Cen J, Zhang L, Wang Z, Xie WF, Li H, Li Y, Hui L, 2019. A homeostatic Arid1a-dependent permissive chromatin state licenses hepatocyte responsiveness to liver-injury-associated YAP signaling. Cell Stem Cell 25, 54–68 e55. [PubMed: 31271748]

Liu C, Tate T, Batourina E, Truschel ST, Potter S, Adam M, Xiang T, Picard M, Reiley M, Schneider K, Tamargo M, Lu C, Chen X, He J, Kim H, Mendelsohn CL, 2019. Pparg promotes differentiation and regulates mitochondrial gene expression in bladder epithelial cells. Nat. Commun. 10, 4589. [PubMed: 31597917]

Margueron R, Reinberg D, 2011. The Polycomb complex PRC2 and its mark in life. Nature 469, 343–349. [PubMed: 21248841]

Neigeborn L, Carlson M, 1984. Genes affecting the regulation of SUC2 gene expression by glucose repression in Saccharomyces cerevisiae. Genetics 108, 845–858. [PubMed: 6392017]

Nie Z, Xue Y, Yang D, Zhou S, Deroo BJ, Archer TK, Wang W, 2000. A specificity and targeting subunit of a human SWI/SNF family-related chromatin-remodeling complex. Mol. Cell Biol. 20, 8879–8888. [PubMed: 11073988]

Papafotiou G, Paraskevopoulou V, Vasilaki E, Kanaki Z, Paschalidis N, Klinakis A, 2016. KRT14 marks a subpopulation of bladder basal cells with pivotal role in regeneration and tumorigenesis. Nat. Commun. 7, 11914. [PubMed: 27320313]

Peterson CL, Herskowitz I, 1992. Characterization of the yeast SWI1, SWI2, and SWI3 genes, which encode a global activator of transcription. Cell 68, 573–583. [PubMed: 1339306]

Robertson AG, Kim J, Al-Ahmadie H, Bellmunt J, Guo G, Cherniack AD, Hinoue T, Laird PW, Hoadley KA, Akbani R, Castro MAA, Gibb EA, Kanchi RS, Gordenin DA, Shukla SA, Sanchez-Vega F, Hansel DE, Czerniak BA, Reuter VE, Su X, de Sa Carvalho B, Chagas VS, Mungall KL, Sadeghi S, Pedamallu CS, Lu Y, Klimczak LJ, Zhang J, Choo C, Ojesina AI, Bullman S, Leraas KM, Lichtenberg TM, Wu CJ, Schultz N, Getz G, Meyerson M, Mills GB, McConkey DJ, Network TR, Weinstein JN, Kwiatkowski DJ, Lerner SP, 2017. Comprehensive molecular characterization of muscle-invasive bladder cancer. Cell 171, 540–556 e525. [PubMed: 28988769]

Schafer FM, Algarrahi K, Savarino A, Yang X, Seager C, Franck D, Costa K, Liu S, Logvinenko T, Adam R, Mauney JR, 2017. Mode of surgical injury influences the source of urothelial progenitors during bladder defect repair. Stem Cell Rep. 9, 2005–2017.

Shin K, Lee J, Guo N, Kim J, Lim A, Qu L, Mysorekar IU, Beachy PA, 2011. Hedgehog/Wnt feedback supports regenerative proliferation of epithelial stem cells in bladder. Nature 472, 110–114. [PubMed: 21389986]

Signoretti S, Pires MM, Lindauer M, Horner JW, Grisanzio C, Dhar S, Majumder P, McKeon F, Kantoff PW, Sellers WR, Loda M, 2005. p63 regulates commitment to the prostate cell lineage. Proc. Natl. Acad. Sci. U. S. A. 102, 11355–11360. [PubMed: 16051706]

Stern M, Jensen R, Herskowitz I, 1984. Five SWI genes are required for expression of the HO gene in yeast. J. Mol. Biol. 178, 853–868. [PubMed: 6436497]

Sun X, Chuang JC, Kanchwala M, Wu L, Celen C, Li L, Liang H, Zhang S, Maples T, Nguyen LH, Wang SC, Signer RA, Sorouri M, Nassour I, Liu X, Xu J, Wu M, Zhao Y, Kuo YC, Wang Z, Xing C, Zhu H, 2016. Suppression of the SWI/SNF component Arid1a promotes mammalian regeneration. Cell Stem Cell 18, 456–466. [PubMed: 27044474]

Tamkun JW, Deuring R, Scott MP, Kissinger M, Pattatucci AM, Kaufman TC, Kennison JA, 1992. brahma: a regulator of Drosophila homeotic genes structurally related to the yeast transcriptional activator SNF2/SWI2. Cell 68, 561–572. [PubMed: 1346755]

Trizzino M, Barbieri E, Petracovici A, Wu S, Welsh SA, Owens TA, Licciulli S, Zhang R, Gardini A, 2018. The tumor suppressor ARID1A controls global transcription via pausing of RNA polymerase II. Cell Rep. 23, 3933–3945. [PubMed: 29949775]

Wang J, Batourina E, Schneider K, Souza S, Swayne T, Liu C, George CD, Tate T, Dan H, Wiessner G, Zhuravlev Y, Canman JC, Mysorekar IU, Mendelsohn CL, 2018. Polyploid superficial cells that maintain the urothelial barrier are produced via incomplete cytokinesis and endoreplication. Cell Rep. 25, 464–477 e464. [PubMed: 30304685]

Wilsker D, Probst L, Wain HM, Maltais L, Tucker PW, Moran E, 2005. Nomenclature of the ARID family of DNA-binding proteins. Genomics 86, 242–251. [PubMed: 15922553]

Zhang X, Shetty M, Clemente V, Linder S, Bazzaro M, 2021. Targeting Mitochondrial Metabolism in Clear Cell Carcinoma of the Ovaries. bioRxiv, 2021.2002.2017.431266.

Zhou P, Zhang Y, Ma Q, Gu F, Day DS, He A, Zhou B, Li J, Stevens SM, Romo D, Pu WT, 2013. Interrogating translational efficiency and lineage-specific transcriptomes using ribosome affinity purification. Proc. Natl. Acad. Sci. U. S. A. 110, 15395–15400. [PubMed: 24003143]

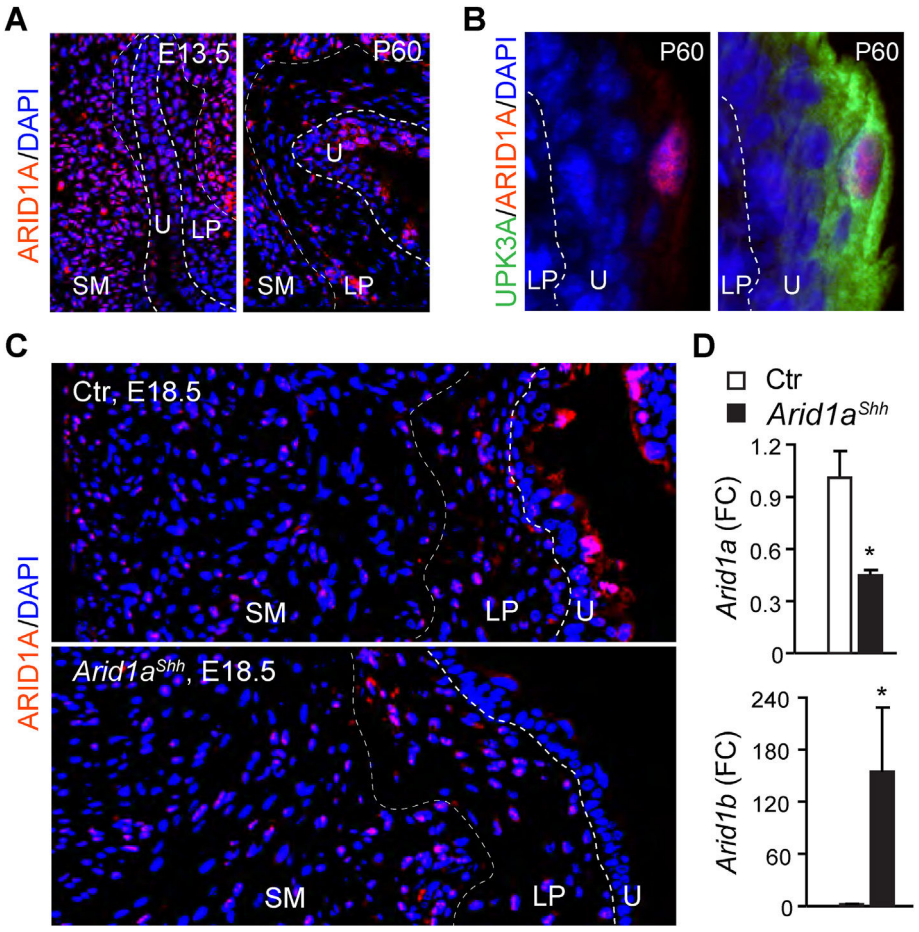

Fig. 1. *Arid1a* is broadly expressed in the developing bladder and enriched in terminally differentiated superficial cells.

(A and B) Immunofluorescence staining of embryonic day 13.5 (E13.5) and postnatal day 60 (P60) bladder sections using Upk3a (green) and Arid1a (red)-specific antibodies. DAPI (blue), nuclear counter staining. White dashed lines demarcate layers of the bladder. U, urothelium; LP, lamina propria; SM smooth muscle. (C) Immunofluorescence staining of bladder sections of E18.5 *Arid1a*^{Shh} and control (Ctr) embryos using Arid1a (red)-specific antibody. (D) qRT-PCR analysis of *Arid1a* and *Arid1b* in micro-dissected bladder urothelium of E18.5 *Arid1a*^{Shh} and control embryos. *Gapdh* was used as an internal control. Data represent mean ± SEM, n = 4. Student's *t*-test. *, $P < 0.05$ vs. Ctr.

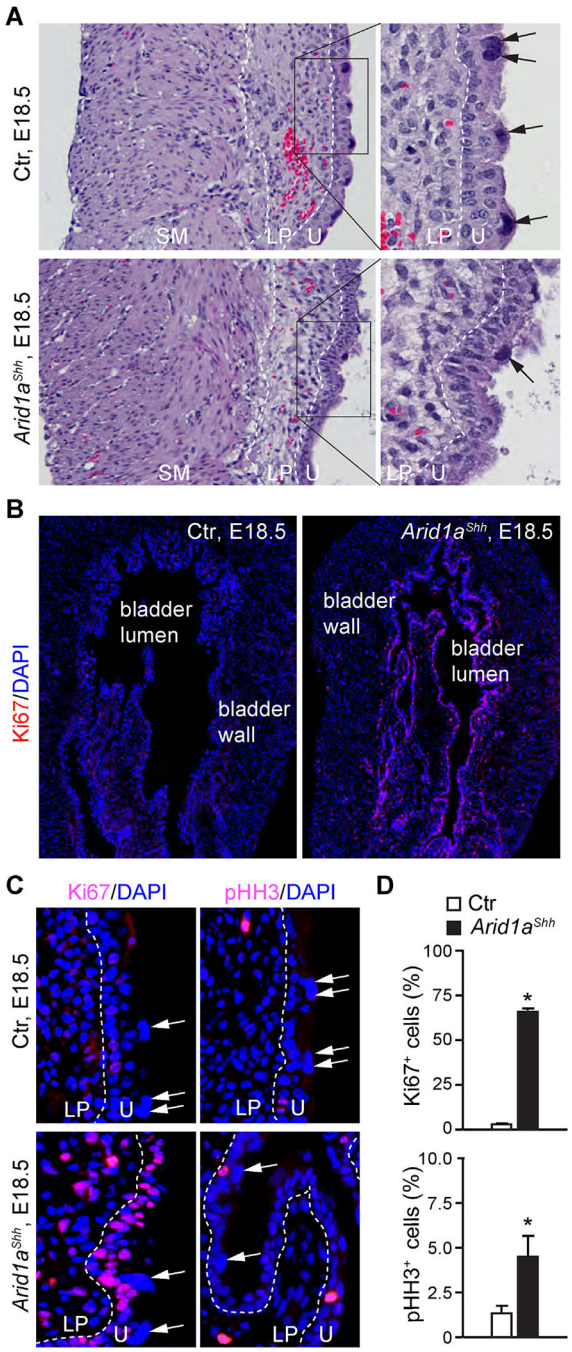

Fig. 2. Arid1a deletion causes hyper-proliferation of the embryonic bladder urothelium.

(A) H&E staining of control (Ctr) and *Arid1a*^{Shh} bladder sections at E18.5. (B and C) E18.5 control and *Arid1a*^{Shh} bladder sections subjected to immunofluorescence staining of proliferating cells using Ki67 (red) or pHH3 (red)-specific antibodies. DAPI (blue), nuclear counter staining. LP, lamina propria; SM, smooth muscle; U, urothelium. (D) Quantification of results shown in B and C. % of urothelial cells. White and black arrows point to the superficial cells. Mean ± SEM, n = 4. Student's *t*-test. *, $P < 0.05$ vs. Ctr.

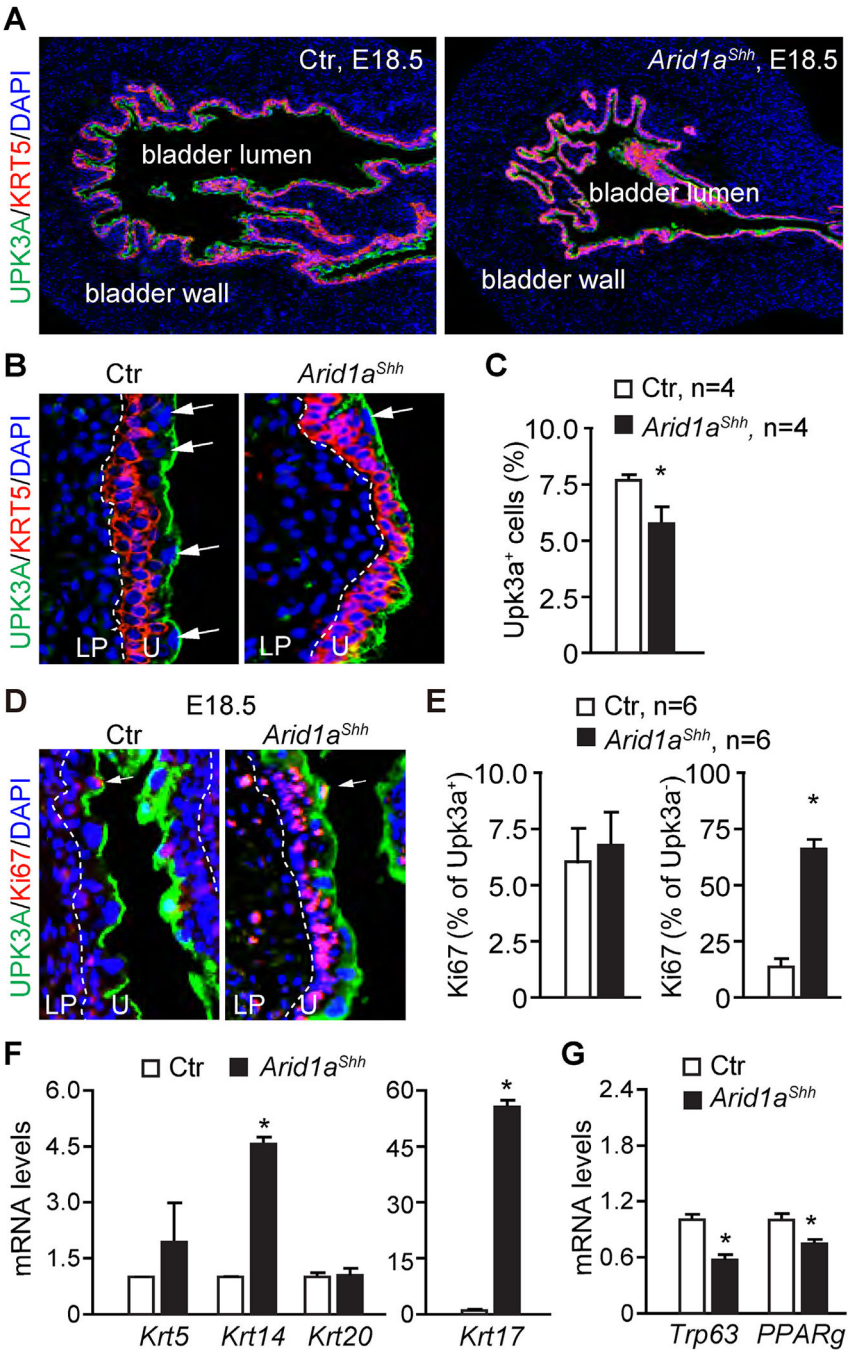

Fig. 3. *Arid1a* regulates bladder urothelial cell differentiation during development.

(A and B) Immunofluorescence staining of embryonic day 18.5 (E18.5) using basal and superficial cell specific antibodies Cytokeratin 5 (Krt5, red) and Uroplakin 3a (Upk3a, green). DAPI (blue), nuclear counter staining. White dashed lines demarcate layers of the bladder. Arrows point to the superficial cells. U, urothelium; LP, lamina propria. (C) Percentage of Upk3^{+} cells in bladder urothelium as shown in A and B. Mean ± SEM, n = 4. Student's *t*-test. *, $P < 0.05$ vs. Ctr. (D and E) co-immunostaining of E18.5 bladder sections using Upk3a (green) and Ki67 (red) antibodies. Quantification of the results shown in E.

Mean ± SEM, n = 6. Student's *t*-test. *, $P < 0.05$ vs. Ctr. (F and G) qRT-PCR analyses of gene transcripts using micro-dissected bladder urothelium of E18.5 *Arid1a*^{Shh} and controls (Ctr). Mean ± SEM, n = 4. Student's *t*-test, *, $P < 0.05$ vs. Ctr.

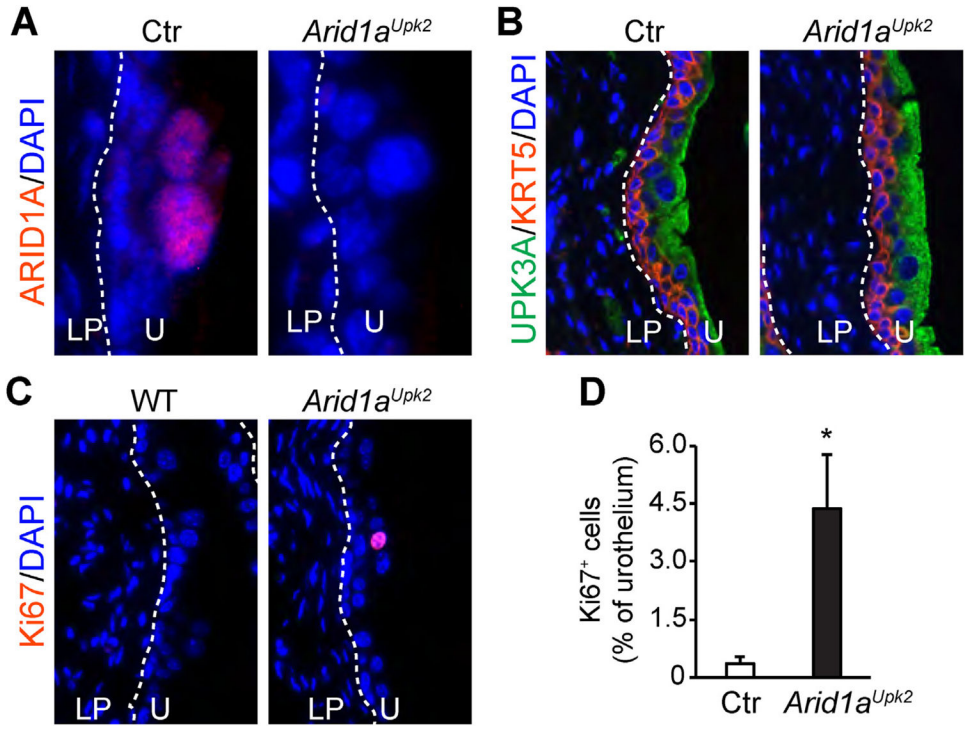

Fig. 4. *Arid1a* is required to maintain the quiescent state of mature urothelium.

(A) Immunostaining of Arid1a (red) of adult bladders of *Arid1a*^{Upk2} and control (Ctr) mice. (B) co-immunostaining of adult bladder urothelium using cell-type specific markers Krt5 (red) and Upk3a (green) specific antibodies. (C and D) Immunostaining of proliferating cells in *Arid1a*^{Upk2} mutant urothelium using Ki67-specific antibody (red). Quantification of Ki67^{+} cells shown in D. *, $P < 0.05$ vs. Ctr, Student's *t*-test, n = 4.

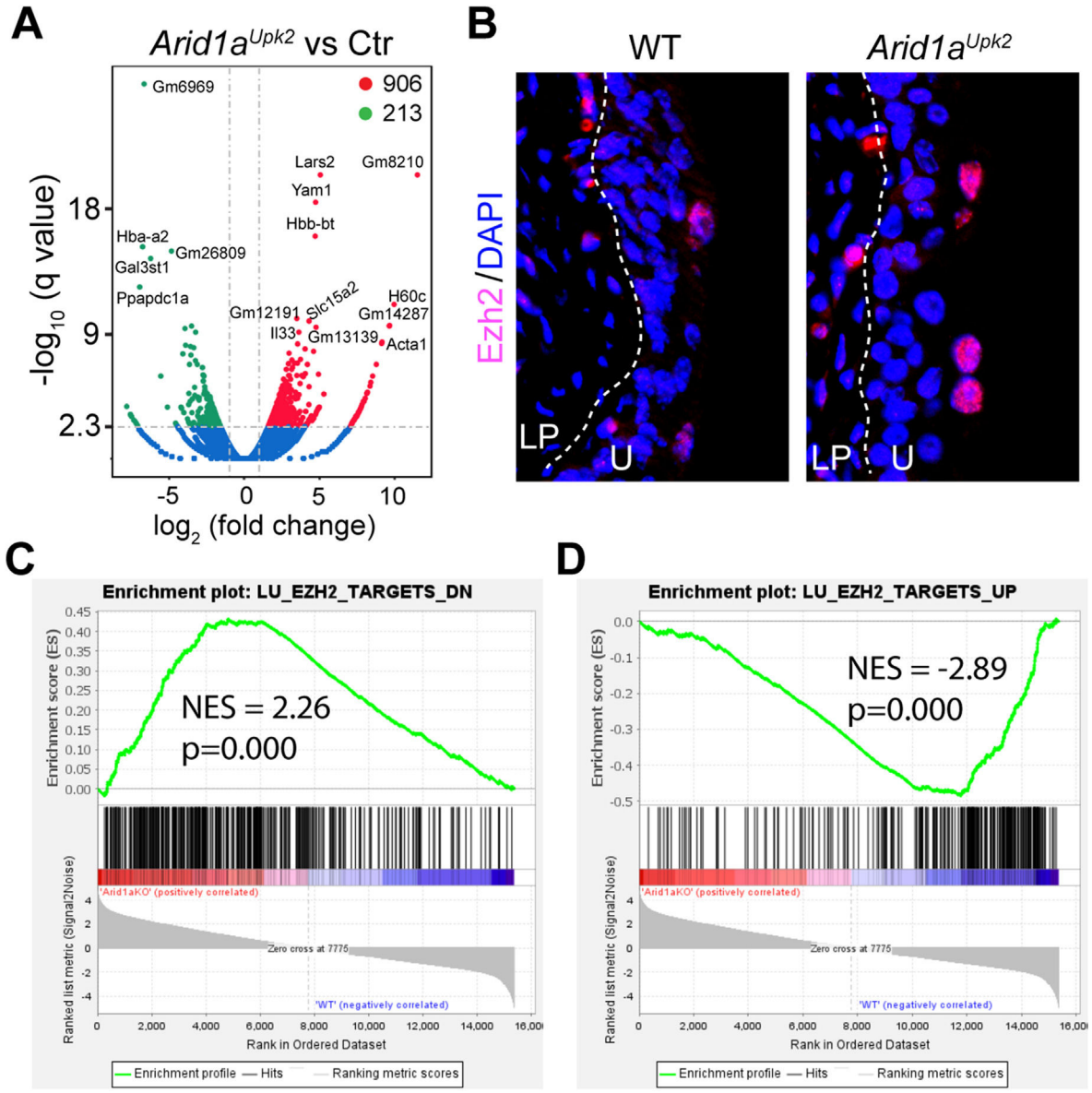

Fig. 5. Deletion of *Arid1a* in mature urothelium causes ectopic expression and activation of *Ezh2*.

(A) Volcano plot of transcriptome of adult bladder urothelium comparing *Arid1a*^{Upk2} to controls (Ctr). (B) Ezh2-specific immunostaining (purple) of adult mouse bladder sections of *Arid1a*^{Upk2} mutants and controls. DAPI, nuclear counter staining. (C–D) Gene Set Enrichment Analysis (GSEA) of differentially expressed genes shown in A using the Ezh2 target gene sets. Down-regulated gene set after *Ezh2* knockdown is shown in C and upregulated gene set after *Ezh2* knockdown is shown in D. NES, net enrichment score.

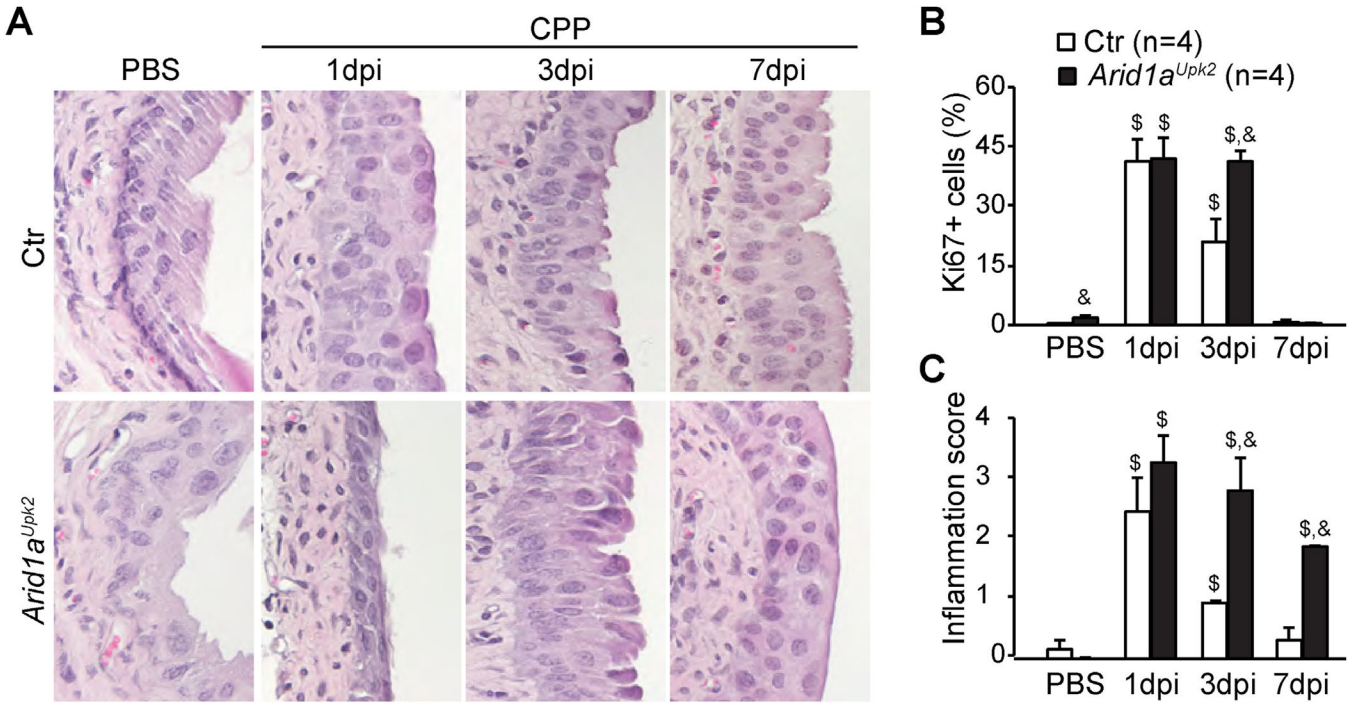

Fig. 6. Urothelium without *Arid1a* is hypersensitive to bladder injury.

(A) H&E staining of bladder sections from heterozygous control (Ctr) and *Arid1a*^{Upk2} mutants. Adult mice were treated with a single dose of cyclophosphamide (CPP) to induce bladder injury or vehicle control (PBS). Bladders were analyzed at day 1, 3 and 7-post-injury (dpi). (B) Quantification of Ki67^{+} proliferating urothelial cells after CPP-induced injuries. (C) Quantification of bladder inflammation induced by acute CPP exposure. Inflammation was scored based on immune cell infiltration, edema, and loss of urothelial cells. Student's t-test; mean ± SEM; \$, $p < 0.05$ compared to PBS; &, $p < 0.05$ compared to Ctr; n = 4.

Table 1

Top 10 Hallmark gene sets enriched in *Arid1a*^{Upk2} mutants compared to wildtype control mice before injury.

ES, enrichment score; NES, normalized enrichment score; positive ES and NES scores, enriched in *Arid1a*^{Upk2}; negative ES and NES scores, enriched in control; NOM p-val, nominal p-value; FDR q-val, false discovery rate (FDR) and q-values.

HALLMARK_GENESET NAME	SIZE	ES	NES	NOM p-val	FDR q-val
MITOTIC_SPINDLE	199	0.43	2.11	0	0
UV_RESPONSE_DN	143	0.44	2.1	0	0
G2M_CHECKPOINT	196	0.42	2.07	0	0
PROTEIN_SECRETION	94	0.41	1.8	0	0.002
E2F_TARGETS	199	0.35	1.75	0	0.004
OXIDATIVE_PHOSPHORYLATION	197	−0.46	−2.59	0	0
XENOBIOTIC_METABOLISM	194	−0.4	−2.23	0	0
COAGULATION	131	−0.38	−2.05	0	0.001
REACTIVE_OXYGEN_SPECIES_PATHWAY	49	−0.45	−1.97	0	0.001
P53_PATHWAY	199	−0.31	−1.82	0	0.003

Table 2

Top 10 Hallmark gene sets enriched in *Arid1a*^{Upk2} mutants compared to wildtype control mice during injury.

ES, enrichment score; NES, normalized enrichment score; positive ES and NES scores, enriched in *Arid1a*^{Upk2}; negative ES and NES scores, enriched in control; NOM p-val, nominal p-value; FDR q-val, false discovery rate (FDR) and q-values.

HALLMARK_GENESET NAME	SIZE	ES	NES	NOM p-val	FDR q-val
MYC_TARGETS_V1	200	0.53	2.33	0	0
MTORC1_SIGNALING	199	0.43	1.85	0	0.002
TNFA_SIGNALING_VIA_NFKB	197	0.42	1.81	0	0.002
INFLAMMATORY_RESPONSE	189	0.42	1.81	0	0.001
MYC_TARGETS_V2	57	0.5	1.76	0	0.003
OXIDATIVE_PHOSPHORYLATION	197	0.4	1.75	0	0.003
IL6_JAK_STAT3_SIGNALING	84	0.44	1.68	0.004	0.006
XENOBIOTIC_METABOLISM	193	−0.52	−1.91	0	0
COAGULATION	134	−0.5	−1.81	0	0.002
BILE_ACID_METABOLISM	111	−0.47	−1.63	0	0.012